



Assessment of Antiangiogenic and Cytotoxic Effects of *Moringa Oleifera* Silver Nanoparticles using Cell Lines

ROLLA AL-SHALABI^{1,2}, NOZLENA ABDUL SAMAD^{1*}, IBRAHIM ALDEEB²,
JULIA JOSEPH¹ and BASSAM M. ABUALSOUD³

¹Department of Toxicology, Sains@BERTAM, Advanced Medical and Dental Institute, Universiti Sains Malaysia, Kepala Batas, Penang, Malaysia.

²Pharmacological and Diagnostic Research Center, Faculty of Pharmacy, Al-Ahliyya Amman University, Al-Salt.

³Department of Pharmaceutics and Pharmaceutical Technology, College of Pharmacy, Al-Ahliyya Amman University, Amman 19328, Jordan.

ABSTRACT

Angiogenesis is the physiological process through which new blood vessels are developed from pre-existing vessels. It includes steps like migration, differentiation, and growth of endothelial cells. Furthermore, it plays a critical role in cancer formation and metastasis. Recently, *Moringa oleifera* (MO) has gained interest due to its properties in various fields, particularly in nanoparticle (NP) technology. This study aims to demonstrate the cytotoxic and antiangiogenic effects of MO silver nanoparticles (MO-AgNPs). Briefly, the cytotoxic effects of MO-AgNPs on Ea. hy 926 and HT 29 cell lines were observed in the Colony Formation Assay. The antiproliferative effects of MO-AgNPs were then further confirmed using MTT assay, in addition to morphological characterization, migration and closure percent calculation. To evaluate the antiangiogenic effect of MO, the chorioallantoic membrane (CAM) assay was done. Fertilized chicken eggs were divided into three groups: MO-AgNPs, MO ethanol extract and negative control. The results showed antiangiogenic effects were observed at 6-12 µg/mL concentration of MO-AgNPs. Whereas the plate efficiency was 45.7 % ± 1%. The surviving fraction at 12, 6, 3, and 1.5 µg/mL was 27.3 ± 0.5%, 30.1 ± 0.5 %, 41.8 ± 1.5%, and 69.8 ± 2.5 %, respectively. MO-AgNPs showed higher cytotoxic activity than MO ethanol extract on the Ea. hy926 cell line, where the IC₅₀ of MO-AgNPs were 74, 35, and 12 µg/mL for 24, 48 and 72 hours, respectively. On the other hand, the IC₅₀ of MO ethanol extract was above 200, 135 and



Article History

Received: 20 July 2024

Accepted: 31 October 2024


Keywords

Antiangiogenic
Cytotoxic;
Moringa Oleifera;
Silver Nanoparticles.

CONTACT Nozlena abdul samad ✉ nozlena@usm.my 📍 Department of Toxicology, Sains@BERTAM, Advanced Medical and Dental Institute, Universiti Sains Malaysia, Kepala Batas, Penang, Malaysia.



© 2024 The Author(s). Published by Enviro Research Publishers.

This is an  Open Access article licensed under a Creative Commons license: Attribution 4.0 International (CC-BY).

Doi: <https://dx.doi.org/10.12944/CRNFSJ.12.1.16>

11 µg/mL for 24, 48 and 72 hours, respectively. Additionally, significant morphological changes were observed in Ea. hy cells. Whereas the closure percent average of Ea. hy cells at 1.5, 3, 6, and 12 µg/mL were 91.603, 88.507, 84.599, and 63.144%, respectively. Based on the results showed in this study, MO extract shows potential to be an effective anti-angiogenic agent and is a promising therapeutic option in cancer treatment.

Introduction

Moringa oleifera (MO) (Family; *Moringaceae*), is a widely distributed angiosperm phytophagous found in many Asian and Southeast Asian countries.¹ *Moringa* is known by many different names depending on the geographic region in which it is grown. For example, it is known as drumstick tree, horse radish tree, or kelor tree.² Importantly, MO plays a critical role in pharmaceutical health care uses, since it has a large variety of compounds that possess high medical and nutritional values. MO is known for its antimicrobial, antioxidant, anti-inflammatory, anti-hypertensive, anti-cancer and wound healing activities.³ The anti-inflammatory and anti-oxidant effects are likely attributed to MO's antiangiogenic effects.⁴ Several studies have documented the antiangiogenic effects of MO's essential oils,⁵ MO's aqueous extract,⁶ and MO's ethanolic extract.⁷ These findings have opened up extensive avenues for medical applications, particularly in the realm of nanotechnology. Nanotechnology underscores the utilization of nanomaterials or zero-dimensional materials, such as nanometallic elements like Au, Ag, Zn, Mg, and Ca, across various disciplines.^{8,9} Of these, silver nanoparticles (AgNPs) are of particular interest owing to their distinctive characteristics, such as good conductivity, chemical stability, catalytic and antibacterial activity. These metal nanoparticles, with a size of less than 50 nm, can carry a large therapeutic dosage due to their large surface area.¹⁰ Nowadays, green synthesis of AgNPs has gained interest because of their benefit in nanomedicine, particularly with MO.¹¹ Green synthesis of MO AgNPs (MO-AgNPs) is safer, eco-friendlier, and less costly to synthesize compared to commercial AgNPs. Thus, it has been used by a number of researchers.¹² In this regard, this study will demonstrate the antiangiogenic effect of MO-AgNPs by using CAM Assay on fertilized eggs and assess the cytotoxicity of MO-AgNPs on human colorectal adenocarcinoma (HT 29) and human umbilical vein endothelial cells (HUVEC) cell lines.

Material and Methods

Phytochemical characterization of Mo Leaf Extract using Hplc-Ms/Ms

The LCMS analysis was done using the Agilent 1290 Infinity LC system coupled to the Agilent 6520 Accurate-Mass Q-TOF mass spectrometer with a dual ESI (electro-spray-ionization) source. The HPLC-MS/MS QTOF analysis was done to analyze the leaf extract of MO. The Agilent Eclipse XDB-C18 Narrow-bore, 150mm x 2.1mm, 3.5-micron (P/N 930990-902) was used as the column with a temperature 25°C and the autosampler temperature of 4°C, with a flow rate of 0.5ml per minute. 3.0µl of the sample was used per injection with both positive and negative polarity. Data were processed with Agilent MassHunter Qualitative Analysis B.07.00.^{13,14}

Nanoparticle Synthesis

The synthesis of silver nanoparticles was carried out using the green synthesis method. A 1% w/v aqueous extract was prepared. 10 mL of the extract was mixed with 90 mL of 1 mM silver nitrate solution. The resulting mixture was then incubated in a water bath at 60°C with agitation for a duration of 8 hours. Subsequently, the nanoparticles were harvested by centrifugation at 6000 RPM for 30 minutes. Following this, the pellet was washed three times with deionized water to remove any residual silver nitrate. The nanoparticles were then freeze-dried and stored at 4°C until further use.¹⁵

Analysis and characterization of MO-AgNPs

UV-Vis Spectrometry

UV-visible spectroscopy is a widely used instrument for analyzing optical properties such as transparency, a gap of the elaborated product, absorption spectroscopy, and reflectance spectroscopy in the ultraviolet and adjacent visible spectral regions (430nm). This band is characteristic of silver nanoparticle formation. An auto-zero is applied to a blank that is inserted prior to adding the sample. The samples were dissolved in deionized water.¹⁶

Dynamic Light Scattering (DLS) Analysis

The DLS analysis of the nanoparticles was done using a nano zeta sizer. This technique showed the relative size distribution of the nanoparticles dispersed in liquid as well as the zeta potential to determine the stability of the nanoparticles in suspension.¹⁷

Cell viability (MTT assay)

The MTT test was used to assess the cell viability of cancer cells. In brief, EA. hy926 and HT 29 cancer cells were seeded into ninety-six-well plates. They were incubated with various concentrations of MO-AgNPs and MO ethanolic extracts (200-12.5 µg/mL) for 24, 48, and 72 hours, respectively.

Each well received an addition of MTT reagent [3-(4,5-dimethylthiazol-2-yl)-2,5-diphenyltetrazolium bromide] (0.5 mg/mL), which was then incubated for 4 hours to allow MTT to be reduced to formazan crystals. A multi-well spectrophotometer (ELISA) plate reader measured the optical density (OD) at 540 and 620 nm wavelengths. Cell viability concentration (IC50 value) was determined. Each experiment was run in triplicate, and results were given as mean ± STD.¹⁵

Morphology and Migration Characterization

To identify the morphology, the endothelial cells EA. hy926 suspension (25×10^4 and 5×10^5) were planted separately in 3 wells in a 6-well plate (Coster Corning, USA) and incubated at 72hr, while the migration characteristics, the EA. hy926 cells were plated in 6-well plates at a density of 5×10^5 cells per well and incubated overnight at 37 °C. The cells were treated with MO-AgNP and incubated for 24, 48, and 72 hr. Morphological characterization was determined by a picture at 0, 24, 48, and 72 hr.¹⁸ Whereas, migration data was analyzed using Motic software version 2 (Motic China group CO, LTD), and closure percent was calculated as follows:

$$\text{Closure percent} = \left(\frac{100 - (\text{Surface area after 24 hr})}{(\text{Surface area at 0 time})} \right) \times 100$$

Colony Formation Assay

In brief, 6-well plates were seeded with 2 mL of EA. hy926 suspension and kept over the night to adhere. Various concentrations of MO-AgNPs (12, 6, 3, and 1.5 µg/mL) were applied. 0.05% DMSO and 0.05% deionized water were employed as

a negative control, and an incubator humidified with 5% CO₂ at 37 °C was used for 72 hours of incubation. Every 3 days, the media was replaced with fresh media, until a minimum of 25 cells had developed in the wells designated as negative controls (approximately 10 days). For colony fixation, 500 µL of 4% paraformaldehyde (Sigma-Aldrich, USA) was applied in each well and kept for an hour. Colonies containing 25 or more cells in each well were counted using a dissecting microscope (Motic, Taiwan) after staining with 500 µL of 0.2% crystal violet solution per well (Sigma-Aldrich, USA). For each intervention, the mean number of colonies was computed.¹⁹

The following formulas were used to calculate the percentages of surviving fraction (SF %) as well as the plating efficiency (PE%)²⁰:

$$\text{PE\%} = \frac{(\text{Number of colonies in negative control}) \times 100}{(\text{Number of seeded } \frac{\text{cells}}{\text{well}})}$$

$$\text{SF\%} = \frac{(\text{Number of colonies in treated well}) \times 100}{(\text{Number of seeded } \frac{\text{cells}}{\text{well}} \times \text{PE\%})}$$

CAM Assay

Fertilized eggs from a chicken farm from Jerash/ Jordan were purchased. All eggs were incubated at 37°C with continuous humidity until new blood vessels are formed. A small needle hole was used to suck the albumin and to separate the Cam from the shell itself. Photos of the eggs were captured before treatment (at zero time) as a standard for comparison purposes, to study the impact of each treatment.

After that, the eggs were split into 3 different groups. The negative control group received only deionized water, the MO-AgNPs group using five eggs was treated with different concentrations of MO-AgNPs (100, 50, 25, 12, and 6 µg/mL respectively), while the MO ethanolic extract group using two eggs was treated with varying concentrations of MO ethanolic extract (100 and 50 µg/mL respectively). The CAM assay results were observed by capturing photos with the same camera that has been used at zero-time documentation to compare the results.²¹

Statistical Analysis

The mean and standard deviation of all the data are presented. P values under 0.05 were considered to have statistical significance when using the non-

parametric Independent Samples Kruskal-Wallis test to determine statistical significance. The software SPSS version 22.0 (SPSS Inc, Chicago, IL) was used for all analyses.

Results and Discussion

In recent years, the use of green synthesis nanotechnology as a part of antiangiogenesis research has given rise to a novel area of study. In this context, MO-AgNPs have garnered increased interest due to their diverse range of toxicological effects.²²

Identification of Major *Moringa Oleifera* Compounds using Hplc-Ms/Ms Qtof Analysis

The chemical identification of MO Compounds using HPLC-MS/MS QTOF analysis revealed major compounds that belong to many chemical groups. However, only compounds that met specific criteria—high scores close to 100, absence in the blank elution, and MFG.ppm values within -2 to +2 were included as main compounds in the results. Major compounds with the highest scores as well as matching data quality, in positive mode were

Ptelatoside A (90.67), Anantine (96.08), C-12 NBD-dihydro-Ceramide (98.1), 5-methyl-octanoic acid (88.69), C16 Sphinganine (97.44), Xestoaminol C (96.18), 16-hydroxy hexadecanoic acid (97.44), 4,5-Di-O-methyl-8-prenylafzelechin-4beta-ol (96.08), TGX-221 (98.18), Hydralazine (89.22), Phenisopham (94.18), while in the negative mode were (R)-Pantolactone (89.69), Merodesmosine (94.4), 4-p-Coumaroylquinic acid (88.26), 2,4-Dichlorobenzoate (89.74), and 3-hydroxy-decanoic acid (91.79) which belongs to carboxylic acids, fatty acids, polyphenolic compounds, alkaloid, pyrrolizidine alkaloid, flavonoids, tannins, steroids, glycosides, amino acid, aspartic acid and glycine.^{23,24} These active ingredients were considered to be responsible for the therapeutic effects of MO-AgNPs owing to their anti-inflammatory and anti-oxidant properties, which are likely contributing to their antiangiogenic effects.⁴

Table 1 shows a List of Compounds from MO leaf extracts using LC-MS/MS analysis illustrating the compounds relative to scores, and MFG ppm.

Table 1: List of Compounds from MO leaf extracts using HP-LC-MS/MS analysis

Molecular	Name Formula	m/z	MS/MS	Error (m/z)	Score (PPM)	RT	Abund
Positive Mode							
C ₁₉ H ₂₆ O ₁₀	Ptelatoside A	432.1861	414.1525	0.35	90.67	1.087	22933.28
C ₁₅ H ₁₅ N ₃ O	Anantine	276.1106	253.1214	0.46	96.08	1.758	31511.41
C ₃₆ H ₆₃ N ₅ O ₆	C-12 NBD-dihydro-Ceramide	679.5123	661.478	-0.31	98.1	9.359	10544.97
C ₉ H ₁₈ O ₂	5-methyl-octanoic acid	181.1202	158.1309	-0.25	88.69	12.089	116767.29
C ₁₆ H ₃₅ N O ₂	C16 Sphinganine	274.274	273.2665	0.84	97.44	12.211	182714.55
C ₁₄ H ₃₁ N O	Xestoaminol C	230.2478	229.2411	0.92	96.18	12.215	105770.07
C ₁₆ H ₃₂ O ₃	16-hydroxy hexadecanoic acid	290.2688	272.2349	0.92	99.22	12.761	777307.63
C ₂₂ H ₂₆ O ₆	4,5-Di-O-methyl-8-prenylafzelechin-4beta-ol	404.2074	386.1732	-0.71	96.08	12.967	71640.02
C ₂₁ H ₂₄ N ₄ O ₂	TGX-221	387.1795	364.1904	-0.45	98.18	12.971	60136.2
C ₈ H ₈ N ₄	Hydralazine	183.0644	160.0752	-0.28	89.22	13.181	66756.8
C ₁₉ H ₂₂ N ₂ O ₄	Phenisopham	343.1645	342.1571	0.42	94.18	13.723	43447.2
Negative Mode							
C ₆ H ₁₀ O ₃	(R)-Pantolactone	129.0557	130.063	-0.23	89.69	4.886	16596.27
C ₁₈ H ₃₄ N ₄ O ₆	Merodesmosine	401.2408	402.2481	-0.54	94.4	7.72	29831.52

$C_{16}H_{18}O_8$	4-p-Coumaroyl -quinic acid	337.0929	338.1	0.62	88.26	8.056	22638.03C7
$H_4C_{12}O_2$	2,4-Dichloro- benzoate	188.9518	189.959	-0.21	89.74	11.646	109109.94\
$C_{10}H_{20}O_3$	3-hydroxy-de canoic acid	187.1337	188.1409	0.3	91.79	12.192	96466.83

Characterization of MO-AgNPs
UV-Vis Spectrometry

The nanoparticle formation was characterized by UV-Vis spectrometry. A distinct broad absorption

band centered around 430 nm became more apparent. This band was a definite indication of the silver nanoparticle formation (MO-AgNPs).

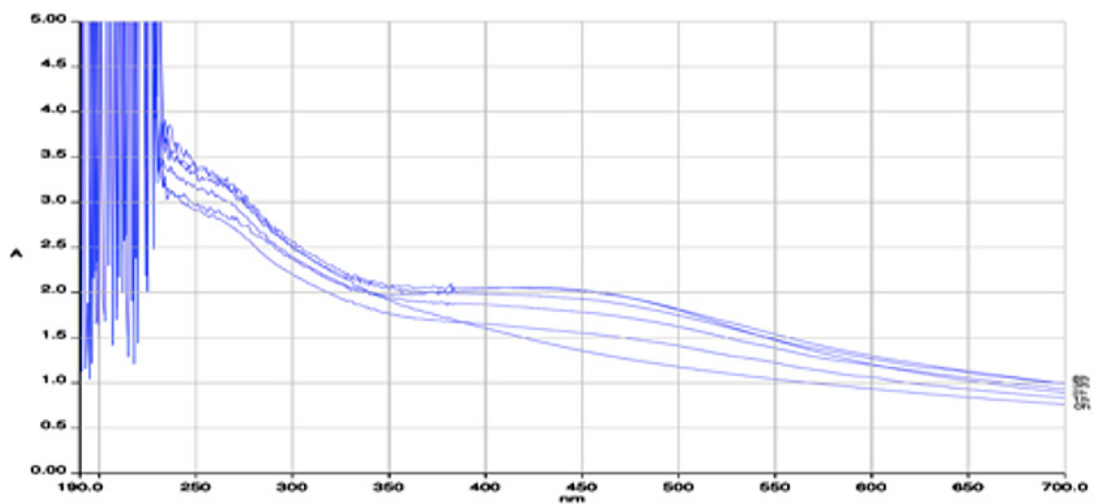


Fig. 1: The UV-Vis spectrometry of MO-AgNPs

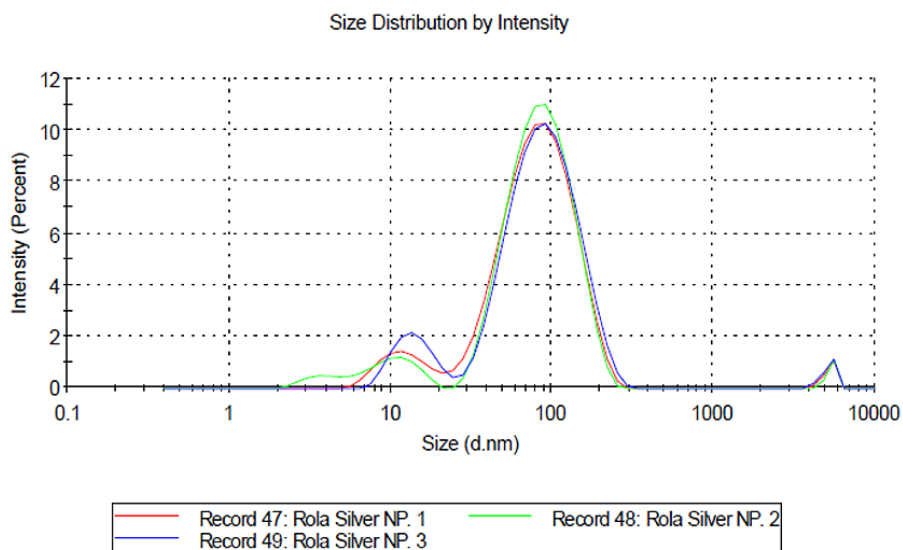


Fig. 2: The size distribution by the number of MO-AgNPs

Dynamic Light Scattering (DLS) Analysis

The DLS analysis of the nanoparticles was performed using a nano zeta sizer. This technique revealed the relative size distribution of liquid-dispersed nanoparticles and their zeta potential, providing insight into suspension stability. The Particle size analyzer (PSA) relied on technologies like high-definition image processing, Brownian motion analysis, gravitational particle seal, and light dispersion. The specific approach utilized laser diffraction, where the angle of light dispersion is inversely related to particle size (i.e. the smaller the particle size, the larger the angle of light scattering). The average particle size was 57.88 nm, with an average PDI of 0.475. MO-AgNPs were categorized

as nanoparticles because their size falls within the range of 10 to 100 nanometers, which is the defining size range for nanoparticles.

Zeta potential, or electrokinetic potential, characterized the charge at the interface between the medium and MO-AgNPs in colloidal dispersion. The electric charge exhibited by the sample particles was termed the zeta value. A negative zeta potential indicated reduced particle aggregation during the continuous process, highlighting the stability of nanoformulations. Investigated samples displayed a -15.9 mV MO-AgNPs zeta potential, signifying moderate suspension stability.

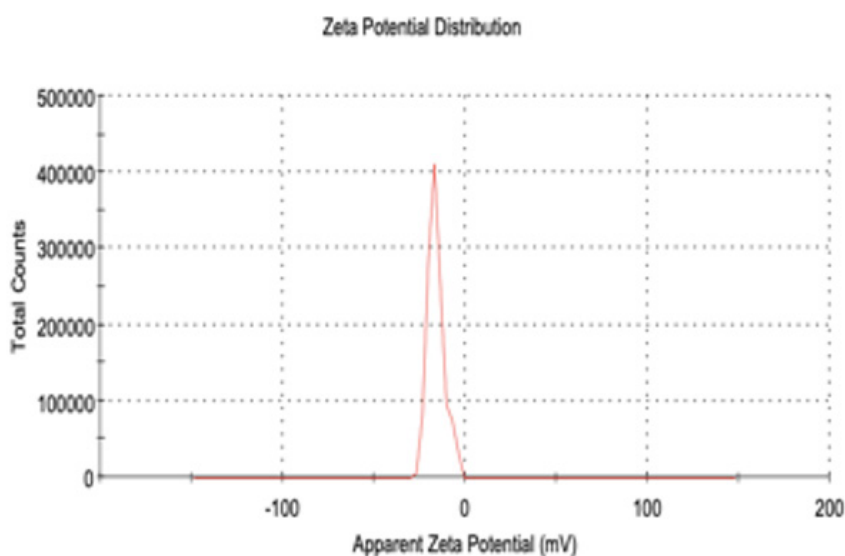


Fig. 3: The Zeta potential distribution of MO-AgNPs

Cell Viability and Anti-Proliferative Effect

IC₅₀ was used to determine the potency of a substance in inhibiting a specific biological or biochemical function by 50%. In this study, cell viability and anti-proliferative properties of MO-AgNP and MO ethanolic extract on both EA. hy926 and HT 29 cell lines were studied using 3-[4,5-dimethylthiazol-2-YL]-2,5-diphenyltetrazolium bromide (MTT) assay. The MO-AgNPs and MO ethanol extract were used in the range of 200- 12.5 µg/mL against EA. hy926 cells for 24, 48, and 72 hr, and results were expressed by IC₅₀ value.

Referring to the results, when comparing the IC₅₀ values, MO-AgNP showed higher cytotoxic activity

against the HT29 cell line compared to MO ethanolic extract with the lowest IC₅₀ values for all timelines tested.

The IC₅₀ of MO-AgNP and MO ethanolic extract on the HT29 cell line after 24 hr was (60, and >200 µg/mL, respectively). Whereas after 48 hr, it was (5.5, and 152 µg/mL, respectively).

Moreover, the results showed the IC₅₀ of MO-AgNPs and MO ethanol extract to be (5.5 and 9) µg/mL, respectively, after 72 hours [Figure 4], which is also the doubling time of the cells.

Therefore, the related IC_{50} of 72 hours was selected to determine the identical IC_{50} of our medication. Thus, it can be concluded that MO-AgNPs have a more cytotoxic effect than MO ethanol extract. This effect was also clear when we used the Ea. hy926 cell line. MO-AgNPs have also showed a

higher cytotoxic activity compared to MO ethanolic extract. The IC_{50} of MO-AgNP was (74, 35, and 12) $\mu\text{g/mL}$ for 24, 48 and 72 hours, respectively. On the other hand, the IC_{50} of MO ethanol extract was (> 200, 135, and 11) $\mu\text{g/mL}$ for 24, 48, and 72 hours, respectively [Figure 5].

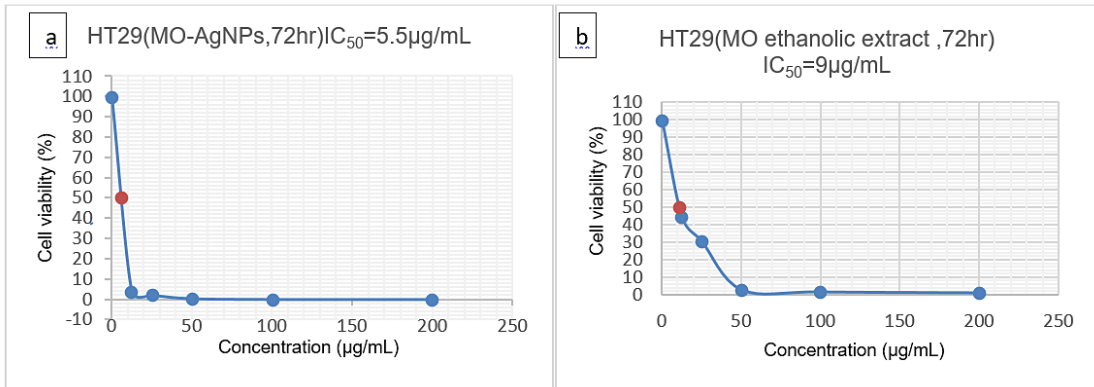


Fig. 4: The cell viability of the HT29 cell line after incubation with MO-AgNP (a) and MO ethanolic extract (b) for 72hr

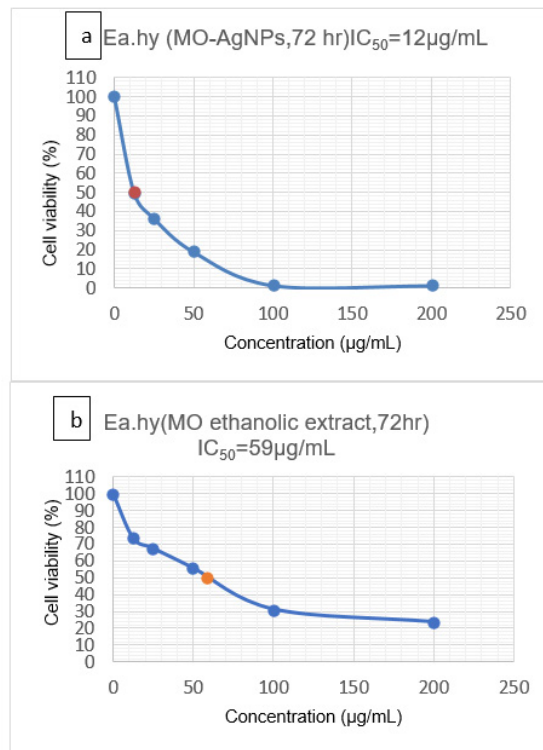


Fig. 5: The cell viability of Ea.hy926 cell line after incubation with MO-AgNP (a) and MO ethanolic extract (b) for 72hr

Figure 6 summarizes the comparison of cell viability of both Ea. hy926 (a) and HT29 (b) cell lines after incubation with MO-AgNP versus MO ethanolic extract for 72h. The findings demonstrate that green production of MO-AgNPs considerably increased

the cytotoxicity of the MO, which may be related to the synergistic interaction between the AgNPs and the natural plant extract's coating on the surface of the NPs.

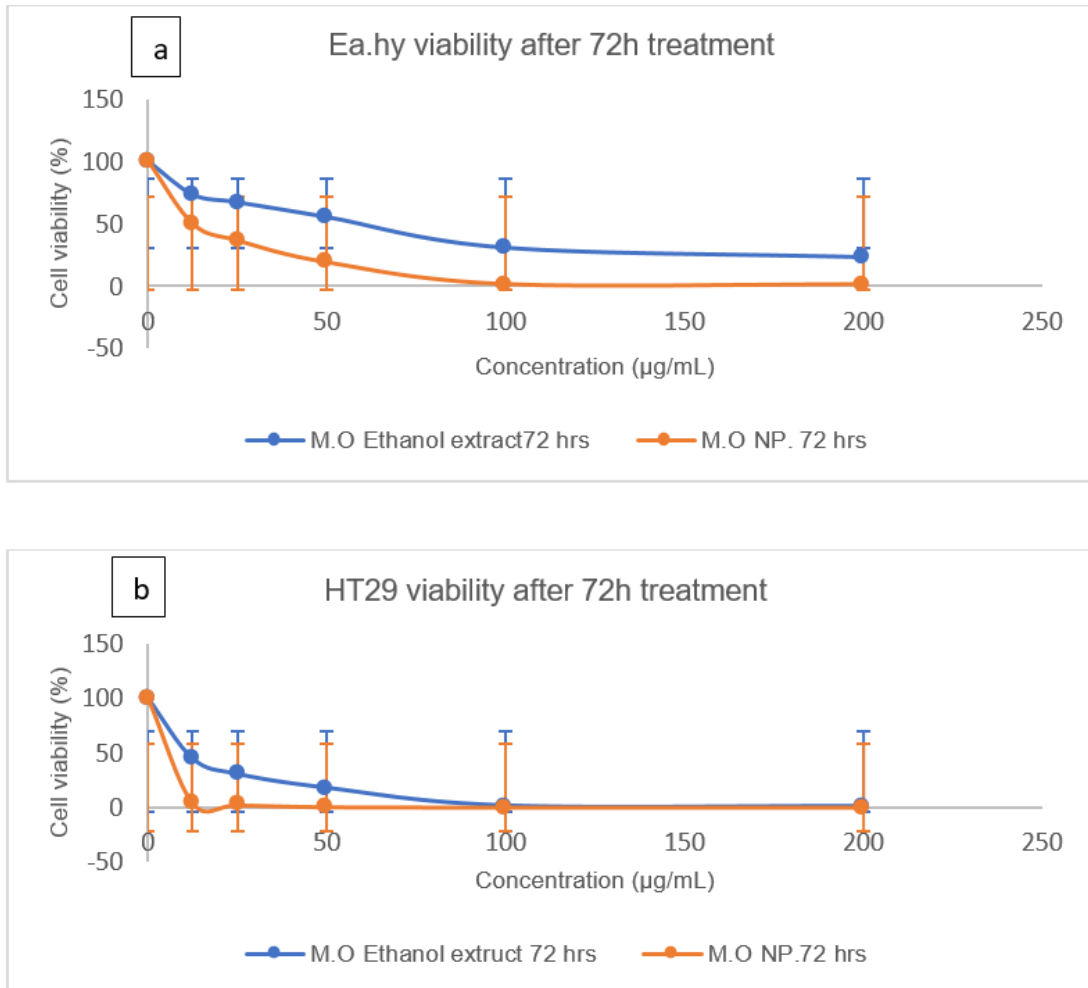


Fig. 6: Comparison of cell viability of Ea.hy926 (a) and HT29 (b) cell lines after incubation with MO-AgNP vs MO ethanolic extract for 72hr

Since the main goal of this research was to study the anti-angiogenic effect of MO, MO-AgNP was chosen for downstream experiments as it has a higher cytotoxic activity than MO ethanol extract against both cell lines. Furthermore, the IC_{50} after 72 hr (5.5 and 12) µg/mL in HT29 and EA.hy926, respectively, were chosen for our further studies to determine the anti-angiogenesis effect of MO.

Morphological and Migration characterization of Mo-Agnps on Ea.hy926 Cell Line after (24, 48 and 72) Hr

Morphology and size are the most critical issues related to the evolution of toxicity.²⁵⁻²⁷ In this study, the effects of MO-AgNP on the morphology and migration of Ea. hy cells were examined. Significant morphological changes were observed in Ea.hy

cells after treatment with MO-AgNPs using their respective IC_{50} values. These changes were increased with time for 24, 48 and 72 hr, respectively

as shown in [Figure 7a, b]. This reflects a clear and significant time-dependent morphological effect for MO-AgNPs.

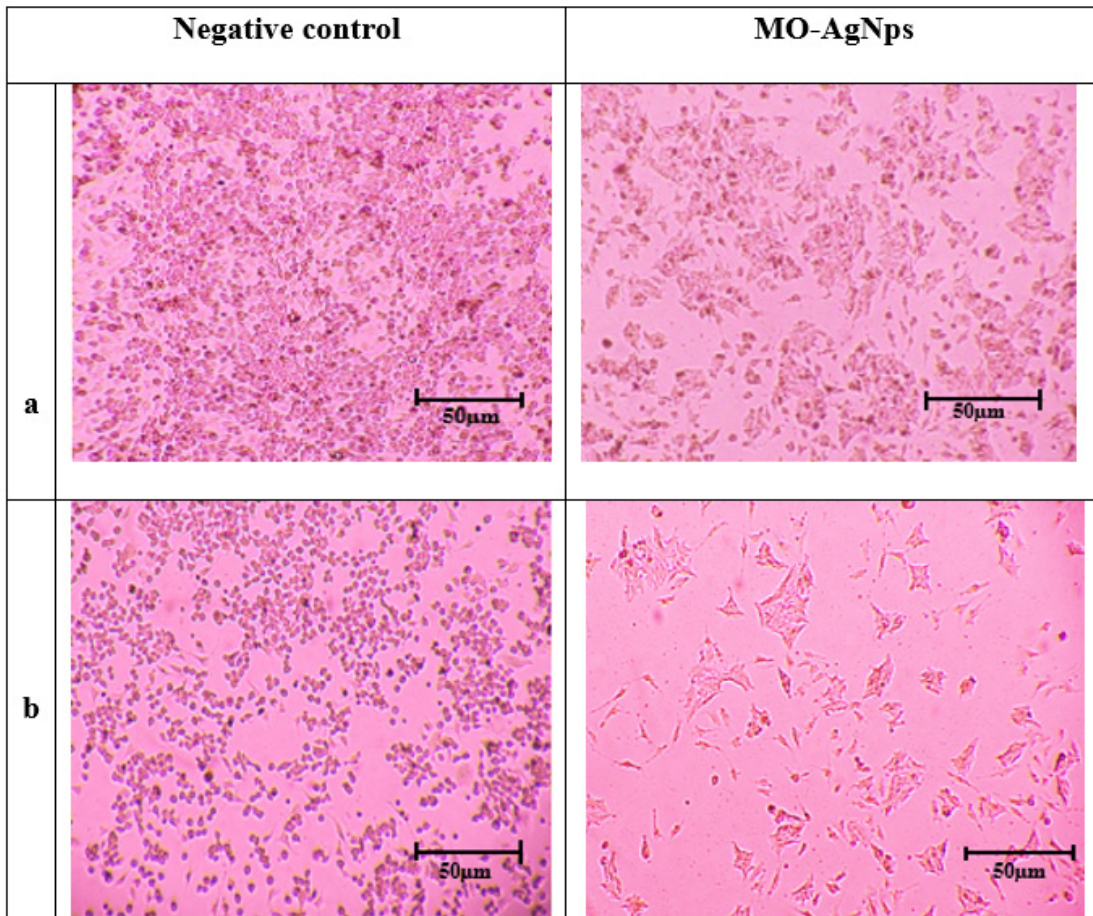


Fig. 7: The cell morphology of EA. hy926 (5×10^5 cells) (figure a) and (25×10^4 cells) (Figure b) after treatment with IC_{50} of MO-AgNPs for 72 hours, under 4x magnification using an inverted microscope

Table II: Closure percent of Ea.hy cells at different concentrations

Conc. Of MO-AgNPs ($\mu\text{g/mL}$)	Average closure percent (%) \pm SD
Negative C	96.875 ± 0.441
12	63.144 ± 1.846
6	84.599 ± 0.708
3	88.507 ± 0.487
1.5	91.603 ± 0.318

Moreover, Ea.hy926 cells showed higher closure percentages at higher concentrations of MO-AgNPs [Figure 8]. The closure percent average of Ea.hy cells at different concentrations (1.5, 3, 6, and 12) $\mu\text{g/mL}$ were (91.603, 88.507, 84.599, and 63.144)% respectively, compared to 96.875 % for negative

control cells [Table II] [Figure 9]. These results were compatible with Khor *et al.* (2018), which showed that MO-NPs caused a significant % of inhibition of Ea.hy cells at (6 and 12) $\mu\text{g/mL}$ were (15.401, and 36.856)% respectively, compared to 3.125 % for negative control cells with IC_{50} doses for 72 hr.²⁸

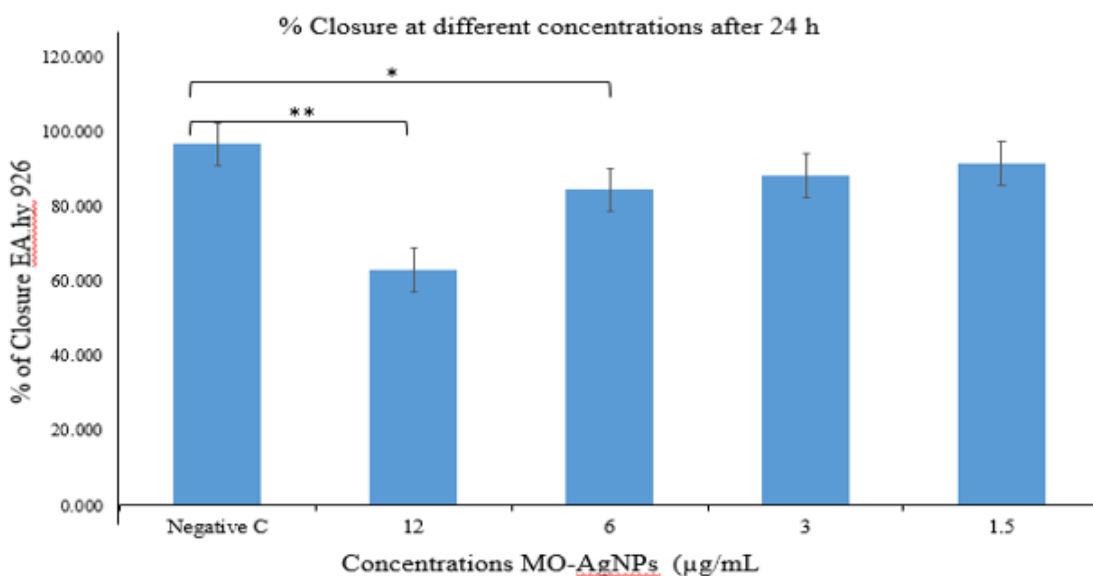
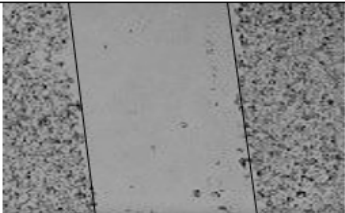
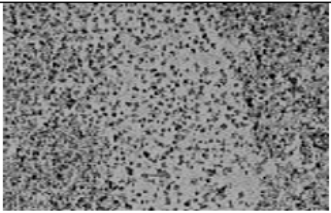
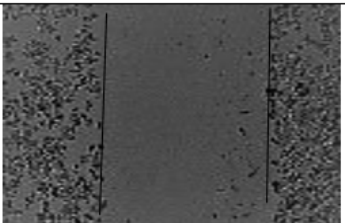
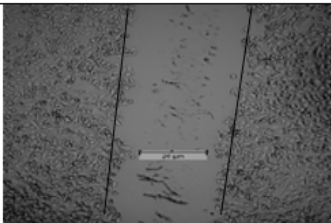


Fig. 8: % Closure using different concentrations of MO-AgNPs. (* $P \leq 0.05$, ** $P \leq 0.01$ Kruskal-Wallis test)

Conc. of MO-AgNPs. ($\mu\text{g/mL}$)	At zero time	After 24 hours
Negative control		
12		

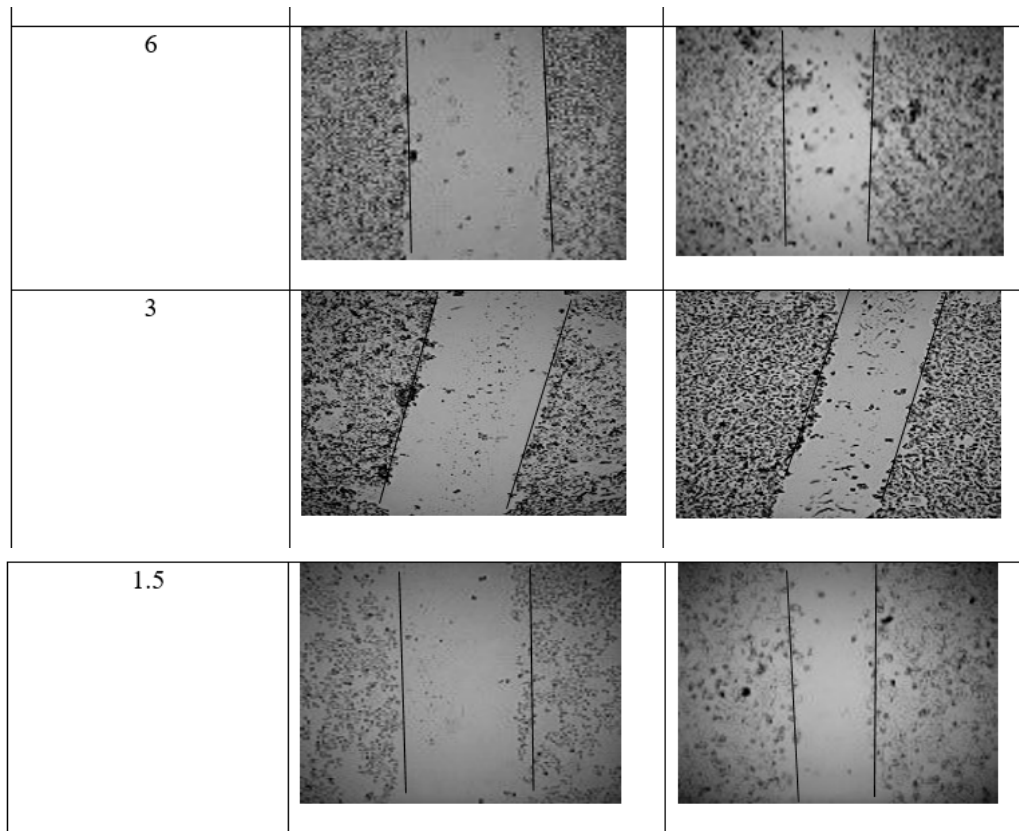


Fig. 9: Images were captured using an inverted microscope at a total magnification power of 4x at both 0 and 24 hours. A solution of 0.05% DMSO and 0.05% deionized water were used as negative control. (Scale; 20 μm).

Cytotoxic effects of MO-AgNPs on EA. hy926 Endothelial Cells Using Cologenic Assay

Four different concentrations of MO were used (12, 6, 3, and 1.5 $\mu\text{g/mL}$). The results of colonogenic assay revealed that MO-AgNPs have anti-proliferative effects on Ea.hy 926 cell line [Table III]. The inhibition percent of MO-AgNPs was (51.5, 49.3, 41.9 and 28.1) % at (12, 6, 3 and 1.5) $\mu\text{g/mL}$, respectively. Thus, the optimal concentration of MO-AgNPs to induce cell death is between (6-12) $\mu\text{g/mL}$.

The PE% (Plate efficiency) was 45.7 % \pm 1%. The surviving fraction at (12, 6, 3, and 1.5) $\mu\text{g/mL}$ was (48.5 \pm 0.5%, 50.7 \pm 0.5 %, 58.03 \pm 1.5%, and 71.9 \pm 2.5 %), respectively.

The findings were expressed compared to the negative control which showed cytotoxicity [Figure 10].

Several previous studies showed similar consequences of MO-AgNPs in cancer cell lines. Sadat Shandiz *et al.* (2017) showed inhibitory activity on cell viability through stimulation of apoptosis in cells of human breast cancer (MCF-7), which provides strong evidence for the MO AgNPs as a promising antiangiogenic drug.²⁹ Furthermore, Vivek *et al.* (2012) showed AgNPs cytotoxicity against MCF-7 and normal breast epithelial cells (HBL-100). The IC₅₀ values observed for AgNPs against MCF-7 and normal HBL-100 cells were as follows: (50 and 30) $\mu\text{g/mL}$ after 24 hours, and (80 and 60) $\mu\text{g/mL}$ after 48 hours of incubation, respectively.³⁰

Effects of Mo-Agnps via the Angiogenesis Mechanistic Pathway using Cam Assay

Commonly, several compounds such as hormones, antibiotics, organo-metallic, and nanoparticles affect

the angiogenesis stimulation or inhibition process in the CAM. Usually, the CAM vascularization development process undergoes three phases.³¹ In the current study, we documented multiple capillary sprouts invading the mesenchyme, forming a major

capillary plexus in all eggs. Antiangiogenic effects of MO-AgNPs was dependent on the concentration used. When MO-AgNPs and MO ethanol extract were tested at different concentrations, phases 2 and 3 was not fully completed.

Table III: Colony formation assay: Surviving fraction % (SF %) and %Inhibition

Concentrations M.O(µg/mL)	SF%	% Inhibition
12	48.5 %	51.5 %
6	50.7%	49.3 %
3	58.03%	41.9 %
1.5	71.9%	28.1 %

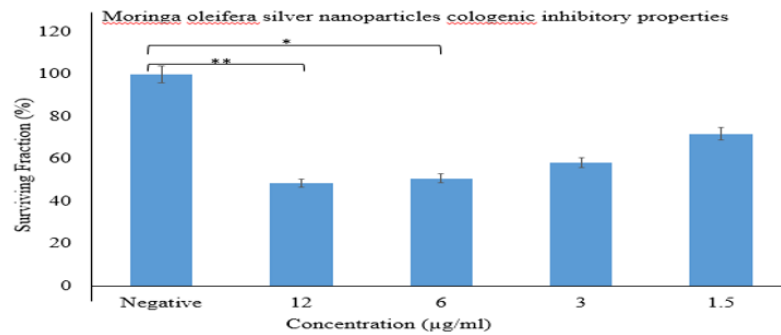


Fig. 10: Colony formation analysis was conducted to determine the SF% of Ea. hy926 cell colonies following a 72-hour exposure to MO-AgNPs at various concentrations (*P ≤0.05, **P ≤0.01 Kruskal-Wallis test).

Conc. of MO-AgNPs & MO Ethanol (µg/mL)	Before Treatment	After Treatment
Negative control		
MO-AgNPs 100 µg/mL		

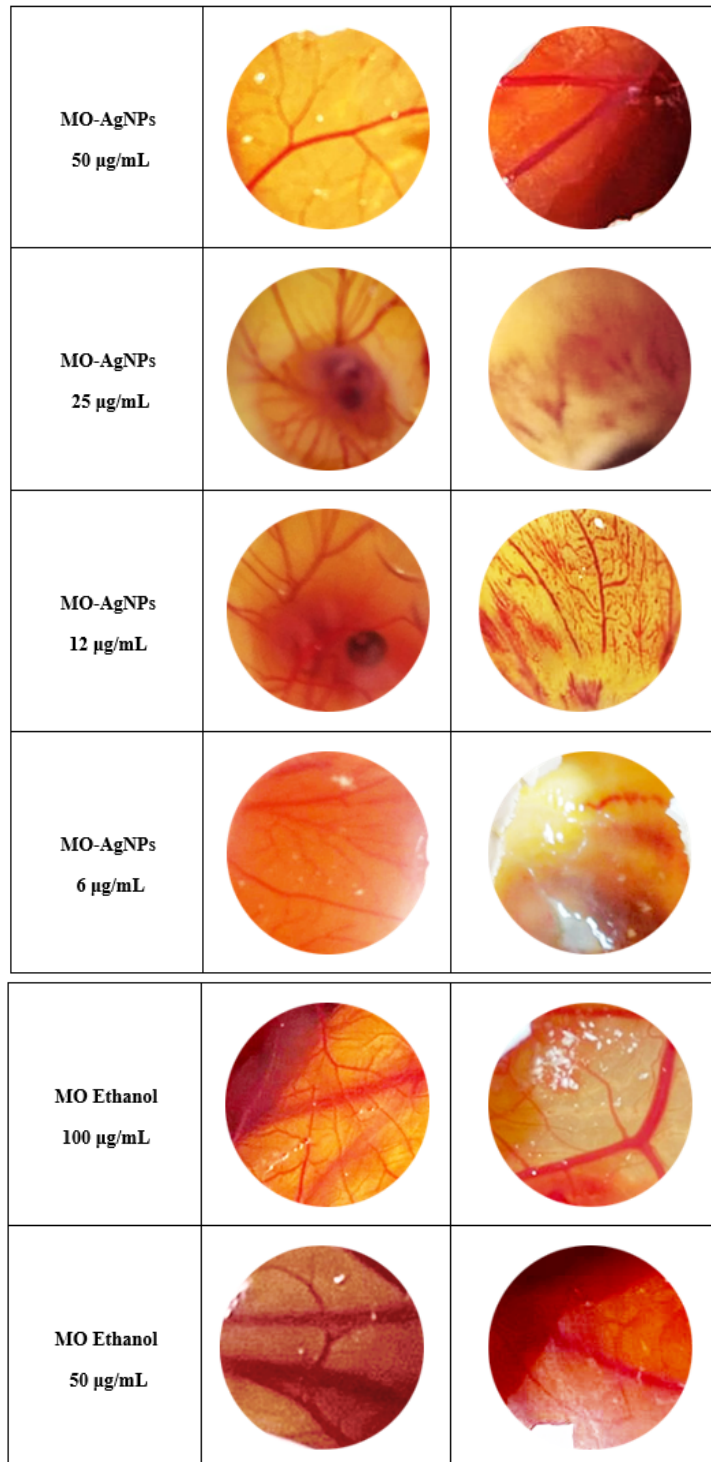


Fig. 11: The images of chorioallantoic membrane (CAM) variants, Candling, Before treatment and after treatment. Main artery exists capillary net and branches are existed or not

In treatment concentrations (25, 12, and 6 µg/mL) the embryo reached the second phase but this phase was not fully completed in different stages with each concentration. Whereas, at the 25 µg/mL concentration, the embryo dies in the early stage of the second phase, as it is clear from the picture which reflects the existence of a small dead embryo surrounded by small individual capillaries [Figure 11]. While in MO-AgNPs (12 µg/mL) the embryo was a little bit larger and the capillary net was more distributed and separated which reflects a clear antiangiogenic effect within this concentration. Another antiangiogenic effect was observed at 6 µg/mL MO-AgNPs concentration which was associated with more growth in embryo size. This result reflects that the suitable antiangiogenic concentration is located between 6-12 µg/mL of MO-AgNPs concentration.

However, at 100 and 50 µg/mL of MO-AgNPs concentration, the embryo stopped developing into phase two and three, which reflects the death of an embryo at an early stage. Similar results (embryonic early death) were noticed with MO ethanol extract concentrations at 100 and 50 µg/mL with differences in stopping the vascularization method compared to MO-AgNPs. Moreover, there is no clear capillary net with MO-AgNPs at 100 and 50 µg/mL compared to MO ethanol extract which showed the existence of capillary net at 100 and 50 µg/mL [Figure 11].

These findings were aligned with several previous studies. Raju & Kei *et al.* (2022) demonstrated that following 24 and 48 hours of treatment, various concentrations of MO leaf extract (50% and 100%) demonstrated a decrease in the blood vessel count in the sample treated region on CAM.⁶ Furthermore, Avram *et al.* reported that in ovo CAM assay for the

antiangiogenesis effect of MO leaves extract (MOLE) has shown a significant reduction in the number of blood vessels. This concludes that MOLE has a potential antiangiogenic effect, which could further contribute to its anticancer activity.³²

Conclusion

This study has shed light on the antiproliferative and cytotoxic effect of MO-AgNPs on Ea. hy 926 and HT 29 cell lines, in addition to the antiangiogenic effect of MO-AgNPs using CAM assay. Findings revealed that the highly effective concentration of MO-AgNPs were at 6-12 µg/mL. Moreover, MO-AgNPs possess a higher cytotoxic effect than MO ethanol extract on the Ea. hy926 cell line. In conclusion, this study adds to the expanding body of evidence supporting MO's promising anti-cancer properties and opens up new possibilities for the therapeutic use of MO extracts for the treatment of colorectal carcinoma and human umbilical vein carcinoma.

Author Contributions

Rolla Al-Shalabi wrote the manuscript, Nozlana Abdul Samad reviewed, edited the manuscript, and supervised the study, Lim Vuanghao and Ibrahim Al-Deeb reviewed and supervised the study, Julia Joseph and Bassam M. Abualsoud reviewed and edited the manuscript.

Acknowledgements

Acknowledgement to Ministry of Higher Education Malaysia for Fundamental Research Grant Scheme with project code: FRGS/1/2020/STG01/USM/03/2

Competing Interests

The authors declare there is no competing interest associated with this work.

References

1. Karimi I. *Moringa oleifera* Lamarck (1785), *Moringaceae* and Cancer I: A Systematic and Comprehensive Review of 24 Years of Research. *Asian Pacific J Cancer Biol.* 2022;7(1):75-96.
2. Matic I, Guidi A, Kenzo M, Mattei M, Galgani A. Investigation of medicinal plants traditionally used as dietary supplements: A review on *Moringa oleifera*. *J Public Health Africa.* 2018;9(3).
3. Milla PG, Peñalver R, Nieto G. Health benefits of uses and applications of *Moringa oleifera* in bakery products. *Plants.* 2021;10(2):318.
4. Marzocco S, Adesso S, Alilou M, Stuppner H, Schwaiger S. Anti-inflammatory and anti-oxidant potential of the root extract

- and constituents of *Doronicum austriacum*. *Molecules*. 2017;22(6):1003.
5. Elsayed EA, Farooq M, Sharaf-Eldin MA, El-Enshasy HA, Wadaan M. Evaluation of developmental toxicity and anti-angiogenic potential of essential oils from *Moringa oleifera* and *Moringa peregrina* seeds in zebrafish (*Danio rerio*) model. *South African J Bot*. 2020;129:229-237.
 6. Kei WW, Shri N, Raju C. Anti-Angiogenic Screening of *Moringa oleifera* Leaves Extract Using Chorioallantonic Membrane Assay. 2022;31(1):225-232.
 7. Dharani S, Pabba S, MadhusudanRao Y. Evaluation of biological activities using ethanolic crude extract of *Moringa oleifera*. *Octa J Biosci*. 2014;2(2).
 8. Mughal B, Zaidi SZJ, Zhang X, Hassan SU. Biogenic nanoparticles: Synthesis, characterisation and applications. *Appl Sci*. 2021;11(6):2598.
 9. Almessiere MA, Slimani Y, Auwal IA, *et al.* Biosynthesis effect of *Moringa oleifera* leaf extract on structural and magnetic properties of Zn doped Ca-Mg nano-spinel ferrites. *Arab J Chem*. 2021;14(8):103261.
 10. Dixit S, Tripathi A. A review on biosynthesis, characterization and antimicrobial effect of silver nanoparticles of *Moringa olifera* (MO-AgNPs). *J Pharm Sci Res*. 2019;11(5):1937-1943.
 11. Kouhbanani MAJ, Beheshtkhoo N, Nasirmoghadas P, *et al.* Green synthesis of spherical silver nanoparticles using *Ducrosia anethifolia* aqueous extract and its antibacterial activity. *J Environ Treat Tech*. 2019;7(3):461-466.
 12. Mehwish HM, Rajoka MSR, Xiong Y, *et al.* Green synthesis of a silver nanoparticle using *Moringa oleifera* seed and its applications for antimicrobial and sun-light mediated photocatalytic water detoxification. *J Environ Chem Eng*. 2021;9(4):105290.
 13. Abdullah AR, Hapidin H, Abdullah H. Phytochemical analysis of *Quercus infectoria* galls extracts using FTIR, LC-MS and MS/MS analysis. *Res J Biotechnol*. 2017;12:12.
 14. Kamaruddin ZH, Sapuan SM, Yusoff MZM, Jumaidin R. Rapid detection and identification of dioscorine compounds in *dioscorea hispida* tuber plants by LC-ESI-MS. *BioResources*. 2020;15(3):5999-6011.
 15. Zi Khor K, Joseph J, Shamsuddin F, Lim V, Moses EJ, Abdul Samad N. The cytotoxic effects of *Moringa oleifera* leaf extract and silver nanoparticles on human kasumi-1 cells. *Int J Nanomedicine*. Published online 2020:5661-5670.
 16. Bindhu MR, Umadevi M, Esmail GA, Al-Dhabi NA, Arasu MV. Green synthesis and characterization of silver nanoparticles from *Moringa oleifera* flower and assessment of antimicrobial and sensing properties. *J Photochem Photobiol B Biol*. 2020;205:111836.
 17. Shousha WG, Aboulthana WM, Salama AH, Saleh MH, Essawy EA. Evaluation of the biological activity of *Moringa oleifera* leaves extract after incorporating silver nanoparticles, *in vitro* study. *Bull Natl Res Cent*. 2019;43(1):1-13.
 18. Mehwish HM, Liu G, Rajoka MSR, *et al.* Therapeutic potential of *Moringa oleifera* seed polysaccharide embedded silver nanoparticles in wound healing. *Int J Biol Macromol*. 2021;184:144-158.
 19. Ibrahim HM, Zaghoul S, Hashem M, El-Shafei A. A green approach to improve the antibacterial properties of cellulose based fabrics using *Moringa oleifera* extract in presence of silver nanoparticles. *Cellulose*. 2021;28:549-564.
 20. Brix N, Samaga D, Hennel R, Gehr K, Zitzelsberger H, Lauber K. The clonogenic assay: robustness of plating efficiency-based analysis is strongly compromised by cellular cooperation. *Radiat Oncol*. 2020;15:1-12.
 21. Vijayakumar S, Chen J, Sánchez ZIG, *et al.* *Moringa oleifera* gum capped MgO nanoparticles: Synthesis, characterization, cyto-and ecotoxicity assessment. *Int J Biol Macromol*. 2023;233:123514.
 22. El-Hak HNG, Moustafa ARA, Mansour SR. Toxic effect of *Moringa peregrina* seeds on histological and biochemical analyses of adult male Albino rats. *Toxicol reports*. 2018;5:38-45.
 23. Tchatchouang S, Beng VP, Kuete V. Antiemetic African medicinal spices and vegetables. In: *Medicinal Spices and Vegetables from Africa*.

- Elsevier*; 2017:299-313.
24. Dong Y, Hao L, Fang K, *et al.* A network pharmacology perspective for deciphering potential mechanisms of action of *Solanum nigrum* L. in bladder cancer. *BMC Complement Med Ther.* 2021;21:1-14.
 25. Teulon JM, Godon C, Chantalat L, *et al.* On the operational aspects of measuring nanoparticle sizes. *Nanomaterials.* 2018;9(1):18.
 26. Hoshyar N, Gray S, Han H, Bao G. The effect of nanoparticle size on *in vivo* pharmacokinetics and cellular interaction. *Nanomedicine.* 2016;11(6):673-692.
 27. Restrepo CV, Villa CC. Synthesis of silver nanoparticles, influence of capping agents, and dependence on size and shape: A review. *Environ Nanotechnology, Monit Manag.* 2021;15:100428.
 28. Khor KZ, Lim V, Moses EJ, Abdul Samad N. The *in vitro* and *in vivo* anticancer properties of *Moringa oleifera*. *Evidence-Based Complement Altern Med.* 2018;2018.
 29. Sadat Shandiz SA, Shafiee Ardestani M, Shahbazzadeh D, *et al.* Novel imatinib-loaded silver nanoparticles for enhanced apoptosis of human breast cancer MCF-7 cells. *Artif cells, nanomedicine, Biotechnol.* 2017;45(6):1082-1091.
 30. Vivek R, Thangam R, Muthuchelian K, Gunasekaran P. Green biosynthesis of silver nanoparticles from *Annona squamosa* leaf extract and its *in vitro* cytotoxic effect on MCF-7 cells. *Process Biochem.* 2012;47(12):2405-2410. doi:10.1016/j.procbio.2012.09.025
 31. Ribatti D. The chick embryo chorioallantoic membrane (CAM) assay. *Reprod Toxicol.* 2017;70:97-101.
 32. Avram S, Ghiulai R, Pavel IZ, *et al.* Phytocompounds targeting cancer angiogenesis using the chorioallantoic membrane assay. *Nat Prod Cancer Drug Discov.* Published online 2017.